

Sensitivity studies using the Weather Research and Forecasting (WRF) model

Sruti Chigullapalli, Prof. Nicole Mölders

The main goal of this research was to find the Weather Research and Forecast model(WRF) configuration best suited for accurately simulating a typical mid March 5-day weather forecast in Interior Alaska. The computational simulation of weather in Alaska is a big challenge due to the low availability of input data because of the vast regions of uninhabited land and dangerous terrain and the complexity of the terrain as well as the extreme climate and light conditions. The purpose of this research was to assess and evaluate the performance of numerical weather predictions from various model configurations, compare the results to the observed data at 22 different weather stations and find the best model configuration. The test cases of WRF were run on midnight and post processing of the data was done using ncl, python and matlab scripts and excel.

Introduction:

The Weather Research and Forecast model (WRF; Skamarock et al. 2005) is the next-generation forecast model and data assimilation system that will advance both the understanding and prediction of weather. It has been designed to support operational forecasting and atmospheric research needs. Moreover, it is suitable for scales ranging from several 100 meters to thousands of kilometers. So far, the model has been tested and evaluated thoroughly mainly in the lower 48s (e.g. Done et al. 2004; Klemp and Skamarock 2004; Knierel et al. 2004; Cheng and Steenburgh 2005; Grell et al. 2005; Davis et al. 2006; Kain et al. 2006) and evaluation for polar regions is limited to short case studies. However, Hines and Bromwich (2008), have developed the Polar WRF and compared its skills with that of Polar MM5 (Bromwich 2001) with simulations over the Greenland ice sheet. Mölders (2008) evaluated WRF over Interior Alaska for a summer episode; Brown (2008) evaluated WRF over the Gulf of Alaska for a winter episode. As the WRF model has not been extensively studied for weather prediction over land in Alaska, it was important to examine which model configuration works best for land by using the ARSC computer as an atmospheric laboratory. Moreover, all the previous research for Alaska involved only one model configuration and this is the first time that over 40 different configurations are being studied for the Alaskan

region. Good numerical forecasts require:

- Initial conditions that adequately represent the state of the atmosphere (three-dimensional wind, temperature, pressure, moisture and cloud parameters)
- A numerical weather prediction model that adequately represents the physical laws of the atmosphere over the whole globe.

The next few sections describe the WRF model components, the various model configurations possible and the results from comparison of some of these simulations.

The WRF Modeling System Program Components

The WRF-ARW model is a fully compressible, nonhydrostatic model. The grid staggering is the Arakawa C-grid. The model uses higher order numerics. These numerics include the Runge-Kutta 2nd and 3rd order time integration schemes, and 2nd to 6th order advection schemes in both horizontal and vertical directions. The dynamics solver conserves scalar variables. The WRF model code contains an initialization programs (metgrid.exe, ungrib.exe, geogrid.exe, real.exe) and a numerical integration program (wrf.exe). WRF I/O API supports NetCDF, PHD5, GriB1 and GriB2 formats as well.

The WRF-ARW model Version 3 that was used for all the simulations discussed in this paper, supports a variety of capabilities. These include:

- Real-data and idealized simulations
- Various lateral boundary condition options for both real-data and idealized simulations
- Full physics options
- Non-hydrostatic and hydrostatic (runtime option)
- Applications ranging from several 100 meters to thousands of kilometers

Program Flow: The program and data flow is schematically shown in Figure 1. The numerical solution of equations that define the atmospheric processes is found by starting with initial conditions and time step towards the solution. For horizontal dynamics, a grid is placed on the model domain, calculating new solutions at each grid point, at each time step. Higher resolution grids tend to yield more accurate results but at a greater computational expense.

For running Real Cases, one would need: WPS + WRF-ARW Model + Post Processing

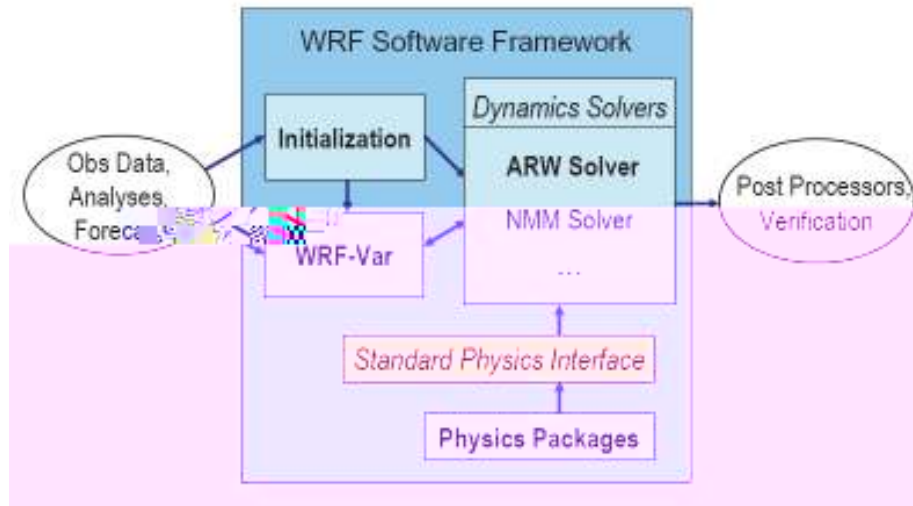


Figure 1: WRF System Components

WRF Model configurations:

In total WRF permits more than 360000 different combinations of physical parameterizations. Of the various physical packages, the ones that were more likely to give good results for the Alaskan region were selected. Table 1 shows the different values used for the various choices of options for treating the cloud microphysics, long and short wave radiation physics, surface layer and boundary layer physics, land-surface atmosphere interaction, and cumulus convection. An exhaustive permutation of these input variables gives a total of 3240 different cases. These were then reduced to 72 from the Arctic point of view, which are shown in Table 2. Of the 72, due to time constraints, only 44 have been analyzed in this paper (added in bold).

Case Number: Each case number starts with the letter WRF and consists of 8 digits. The first 2 digits are for the multi-physics option. These can be one of 05, 06, 08 and 10 depending on the micro-physics scheme used. The third and fourth digits represent the schemes for long and short wave radiation respectively. These are chosen to be 12 or 33. The fifth, sixth and seventh digits together determine the surface layer, land-surface and boundary layer models used. These were chosen to be 222, 232 or 777 in our analysis. The last digit takes the value of the input variable 'cumulus' which can be 1, 2 or 5. An example of a case number is WRF05127771. The 72 cases are numbered such that the eighth digit varies most and the first digit varies least as we go down the list.

Table 1: Different physics options and the scheme used for the project

microphysics mp_physics	5	Ferrier (new Eta) microphysics
	6	WSM 6-class graupel scheme
	8	Thompson scheme
	10	Morrison (2 moments)
Longwave radiation ra_lw_physics	1	rrtm scheme
	3	cam scheme
shortwave radiation ra_sw_physics	2	Goddard short wave
	3	cam scheme
surface-layer sf_sfclay_physics	2	Monin-Obukhov (Janjic) scheme
	7	Pleim-Xiu surface layer (ARW only)
land-surface sf_surface_physics	2	Unified Noah land-surface model
	3	RUC land-surface model
	7	Pleim-Xiu LSM (ARW)
boundary-layer bl_pbl_physics	2	Mellor-Yamada-Janjic TKE scheme
	7	ACM2 (Pleim) PBL (ARW)
cumulus cu_physics	1	Kain-Fritsch (new Eta) scheme
	2	Betts-Miller-Janjic scheme
	5	Modified Grell-Devenyi ensemble scheme

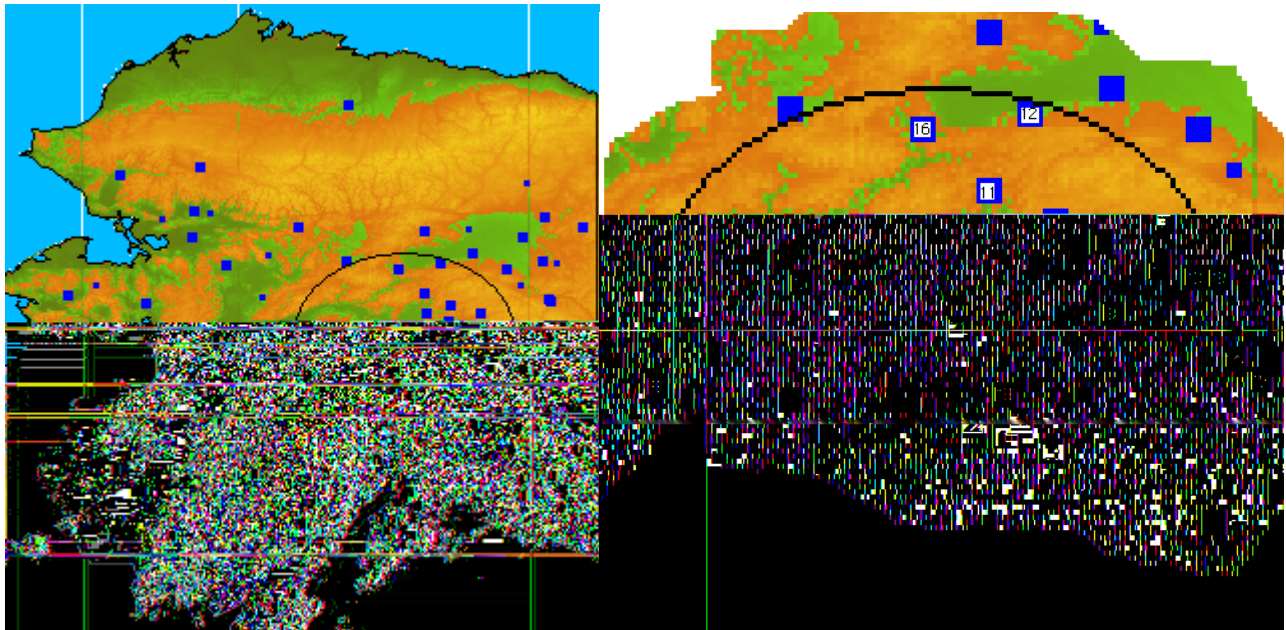
Different physics packages for WRF were evaluated with a 5 day period simulations starting March 13th 2008 that show variable forecast skill when verified with the automatic weather station observations. Through the first six weeks of my internship, I successfully built the WRF case from the source code and learned to submit jobs onto Midnight, a supercomputer at ARSC. We also performed 44 different case studies that include different types of microphysics, long and short wave radiation physics, land surface and boundary layer models. Simulations were performed either by me or Mölders. Ncl and Matlab scripts were used to extract weather data at specific locations in the domain from the NetCDF output files and calculate the statistical averages, errors, respectively.

Table 2: Total list of WRF model configurations and the ones analyzed in this paper (bold).

Case No.	Configuration	Case No.	Configuration	Case No.	Configuration
1	WRF05122221	25	WRF06127771	49	WRF08332321
2	WRF05122222	26	WRF06127772	50	WRF08332322
3	WRF05122225	27	WRF06127775	51	WRF08332325
4	WRF05122321	28	WRF06332221	52	WRF08337771
5	WRF05122322	29	WRF06332222	53	WRF08337772
6	WRF05122325	30	WRF06332225	54	WRF08337775
7	WRF05127771	31	WRF06332321	55	WRF10122221
8	WRF05127772	32	WRF06332322	56	WRF10122222
9	WRF05127775	33	WRF06332325	57	WRF10122225
10	WRF05332221	34	WRF06337771	58	WRF10122321
11	WRF05332222	35	WRF06337772	59	WRF10122322
12	WRF05332225	36	WRF06337775	60	WRF10122325
13	WRF05332321	37	WRF08122221	61	WRF10127771
14	WRF05332322	38	WRF08122222	62	WRF10127772
15	WRF05332325	39	WRF08122225	63	WRF10127775
16	WRF05337771	40	WRF08122321	64	WRF10332221
17	WRF05337772	41	WRF08122322	65	WRF10332222
18	WRF05337775	42	WRF08122325	66	WRF10332225
19	WRF06122221	43	WRF08127771	67	WRF10332321
20	WRF06122222	44	WRF08127772	68	WRF10332322
21	WRF06122225	45	WRF08127775	69	WRF10332325
22	WRF06122321	46	WRF08332221	70	WRF10337771
23	WRF06122322	47	WRF08332222	71	WRF10337772
24	WRF06122325	48	WRF08332225	72	WRF10337775

Methodology:

The grid was centered at Fairbanks. The days March 13th to March 18th were chosen because these dates have approximately equal length of day and night. Each case consists of five day simulations starting at 00 United Time Coordinated (UTC). This refers to 3:00 PM on March 12th in Fairbanks, Local Standard Time (LST). Instead of running the entire 5 day simulation in one shot, we did it in parts using restart files for each day. Multiple physics package options allow flexibility in treating the earth surface, atmospheric boundary layer, shortwave and long-wave radiation, and subgrid scale cumulus clouds. An important consideration for WRF simulation in region around Fairbanks is the selection of physical parameterizations best suited for Alaskan conditions.



*Figure 2: The Map of Alaska showing AWS by blue dots (left).
Enlarged map showing the locations of the 22 stations from Table 1 (right).*

The land surface is treated with either the 4-layer Noah land surface model (LSM) or the 6-layer Rapid Update Cycle (RUC) LSM or the 2-layer Pleim-Xiu LSM. The RUC scheme includes frozen soil, fractional snow cover, and up to two snow layers (Smirnova et al. 1997, 2000). The LSM now commonly referred to as Noah, the name evolved from the earlier acronym NOAH combining NCEP, Oregon State University, Air Force, and Hydrologic Research Laboratory, is based on the Oregon State University LSM (Chen and Dudhia 2001) and includes predicted soil ice, and fractional snow cover characteristics. The Pleim-Xiu LSM bases on the ISBA (Noilhan and Planton 1989) a Force-Restore Model with its modifications by Xiu and Pleim (1995, 2003) and Pleim and Xiu (2001).

The grid is a polar projection centered at $64^{\circ}\text{N } 50'$, $147^{\circ} 36' \text{ W}$ consisting of 150 points in the east–west direction and 110 points in the north–south direction. The time-step is 24 seconds and the length and width of each grid cell is 4 km. For validation, automatic weather station (AWS) data are readily available from the Western Regional Climate Center webpage. Twenty two AWS sites, shown in Table 3, produced useful data for this study.

Table 3: The locations of the 22 weather station at which the observed data was gathered.

	<u>STATION</u>	<u>LATITUDE</u>	<u>LONGITUDE</u>	<u>HEIGHT</u>
1	Angel Creek	65° 01' 12"	146° 13' 41"	1100 ft.
2	Bolio	63° 52' 00"	145° 50' 00"	2450 ft.
3	Caribou Peak	65° 11' 21"	147° 30' 01"	1575 ft.
4	Chatanika	65° 01' 00"	148° 35' 00"	1450 ft.
5	Dunkle Hills	63° 16' 03"	149° 32' 21"	2850 ft.
6	Eielson Visitor Center	63° 25' 53"	150° 18' 34"	3730 ft.
7	Fairbanks	64° 50' 12"	147° 36' 54"	454 ft.
8	George Creek	63° 50' 15"	144° 21' 01"	1525 ft.
9	Gold King	64° 24' 16"	148° 27' 44"	556 ft.
10	Goodpasture	64° 14' 17"	145° 16' 01"	1520 ft.
11	Livengood	65° 25' 25"	148° 43' 18"	450 ft.
12	Lost Creek	66° 02' 33"	147° 58' 17"	700 ft.
13	Manchu	64° 42' 00"	147° 01' 00"	671 ft.
14	Oklahoma	64° 01' 18"	146° 15' 08"	1587 ft.
15	Round Lake	64° 41' 05"	153° 56' 24"	570 ft.
16	Seven Mile	65° 56' 18"	149° 51' 18"	823 ft.
17	Small Arms Range	64° 48' 00"	147° 37' 00"	490 ft.
18	Stampede	63° 44' 52"	150° 19' 41"	1900 ft.
19	Stuart Creek	64° 43' 08"	146° 30' 16"	1543 ft.
20	Toklat	63° 31' 27"	150° 02' 36"	3100 ft.
21	Wein Lake	64° 18' 54"	151° 05' 00"	1050 ft.
22	Wonder Lake	63° 29' 25"	150° 52' 17"	2120 ft.

The 5-day simulations were performed using the restart option for each day after the first day. Each 1 day simulation took an average of 3 hours and hence, each WRF case took about 15 hours of computational time on midnight, a super computer at Artic Region Supercomputing Center, ARSC. The statistics, including correlation of the time variations, bias, and root mean- square error (rmse) were calculated by averaging over all available time over all sites.

Results:

The observed and simulated data for the variables such as solar radiation, mean air temperature, dew point temperature, relative humidity, average wind speed and total precipitation are compared and the correlation skill score and root mean square error are calculated over the entire 5-day period across the 22 stations. Apart from this, a third qualitative skill score called the 'bias' is calculated. This quantity tells us the inherent biased nature of the particular model, that is, if it underestimates or overestimates a certain quantity and by how much. However, positive and negative differences may cancel each other out.

Correlation Coefficient:

If X and Y represent the simulated data and observed data respectively,

$$Corr = \frac{\overline{xy} - \bar{x}\bar{y}}{\sqrt{\overline{x^2} - \bar{x}^2} \sqrt{\overline{y^2} - \bar{y}^2}} \quad \text{where } \bar{x} = \frac{1}{n} \sum_{i=1}^n x_i \text{ is the mean of the data X.}$$

The correlation is 1 in the case of an increasing linear relationship, -1 in the case of a decreasing linear relationship, and some value in between in all other cases, indicating the degree of linear dependence between the variables. The closer the coefficient is to either -1 or 1 , the stronger the correlation between the variables.

Root Mean Square Error and Bias:

If X and Y represent the simulated data and observed data respectively,

$$Rmse = \sqrt{\frac{\sum_{i=1}^n (x_i - y_i)^2}{n}}, \quad Bias = \frac{\sum_{i=1}^n x_i - y_i}{n}$$

The root mean square error is a frequently-used measure of the differences between values predicted by a model and the values actually observed from the thing being estimated. These individual differences are also called residuals, and the RMSE serves to aggregate them into a single measure of predictive power. A positive value of bias for a particular quantity implies that the model over-predicts the quantity. Similarly a negative value implies that it is inherent in the model to under-predict that particular quantity.

The model with least Rmse and highest Correlation factor for each of the above mentioned quantities is considered the best. A larger bias implies that the errors are systematic errors which can be caused due to misinterpretation of landscape or other models. Usually, the lower the Rmse, the better is the model and the closer the bias is to 0, the better. The various sources of error in numerical weather predictions are errors in initial conditions, errors in the model, intrinsic predictability limitations and random or systematic errors.

It has been observed that changing only the cumulus but having all other input variables constant changes the correlation factor and rmse by an order of magnitude of 10^{-3} . Due to the numbering of the cases, the clusters found in the plots are from adjacent case numbers.

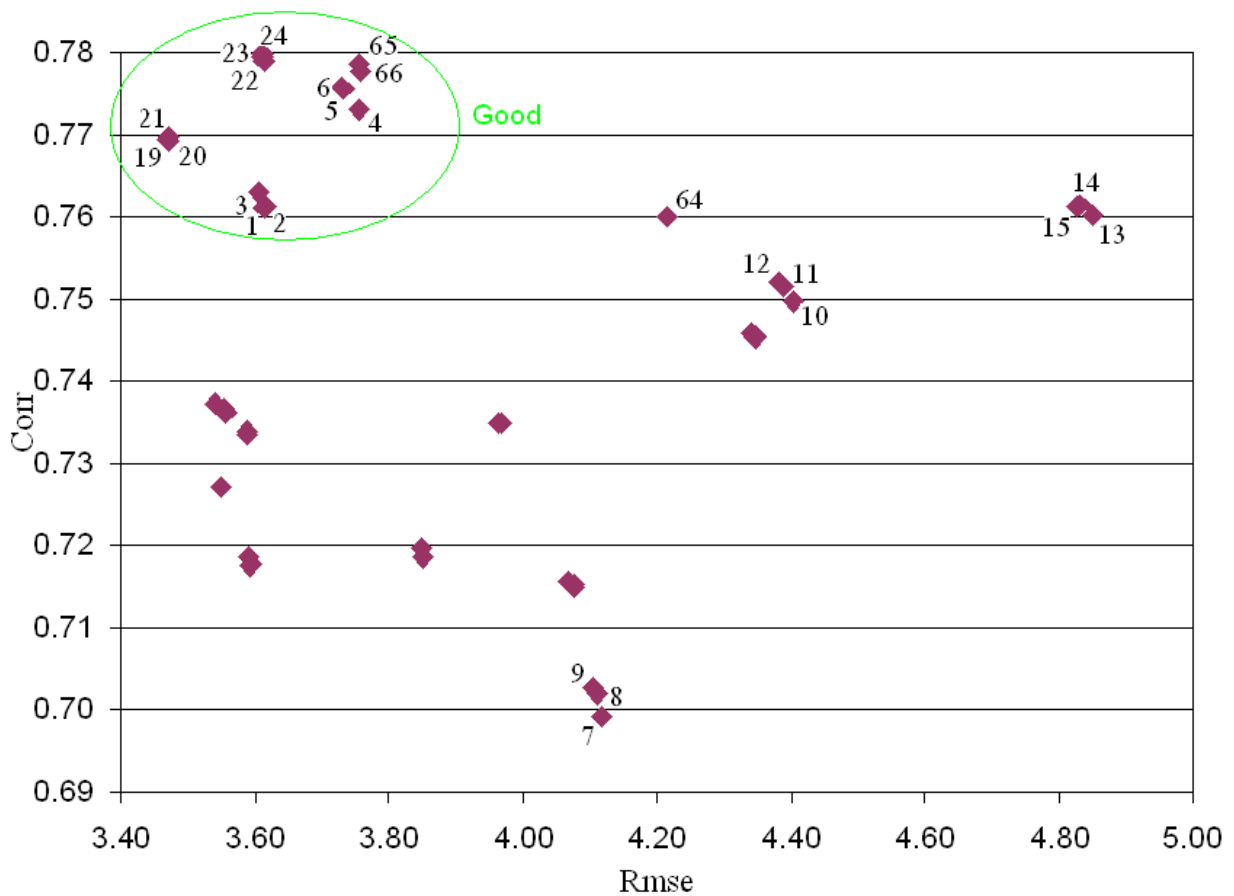


Figure 3: Plot of Correlation factor vs Root Mean Square Error (Rmse) for Air Temperature.

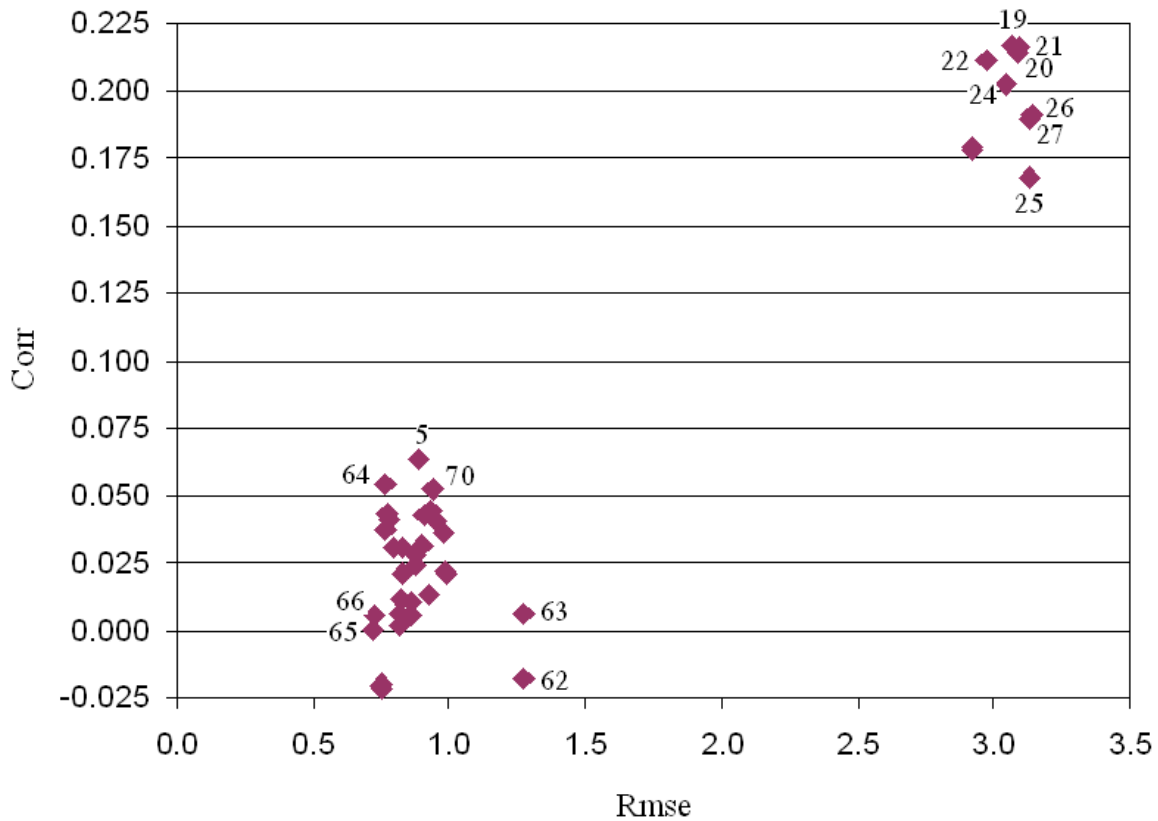


Figure 4: Plot of Correlation factor vs Root Mean Square Error (mm) for Total Precipitation.

From figures 3 and 4, it can be seen that cases 19, 20, 21 and 23, 24, 25 show high correlation and a relatively low Rsme in air temperature. However, these have a correlation factor of ~ 0.2 only and an Rsme of 3mm precipitation which is not very low. Similarly cases 1, 2, 3 and 4, 5, 6 show good results for air temperature, but correlate poorly when it comes to total precipitation. Typically, in March there is very little precipitation observed in Alaska (< 1 inch; Shulski and Wendler 2007). Thus, a judgment for precipitation is difficult. This can also be seen in Fig. 4.

Table 4: Case numbers for the best and worst prediction of each of the physical quantities.

Property	Best Cases	Worst Cases
Shortwave Radiation	16,17,18,65,70	1,2,3,4,5,6,62,63
Average Wind Speed	10,11,12,28,29,30,64,65,66	4,5,6,7,8,9,22,23,24
Air Temperature	1,2,3,4,5,6,19,20,21,22,23,24,65,66	7,8,9,13,14,15
Dew Point Temperature	19,20,21,22,23,24,65	62,63
Relative Humidity	7,8,9,16,17,18,25,26,27,43,44,45	10,11,12,64,65
Total Precipitation	NA	NA

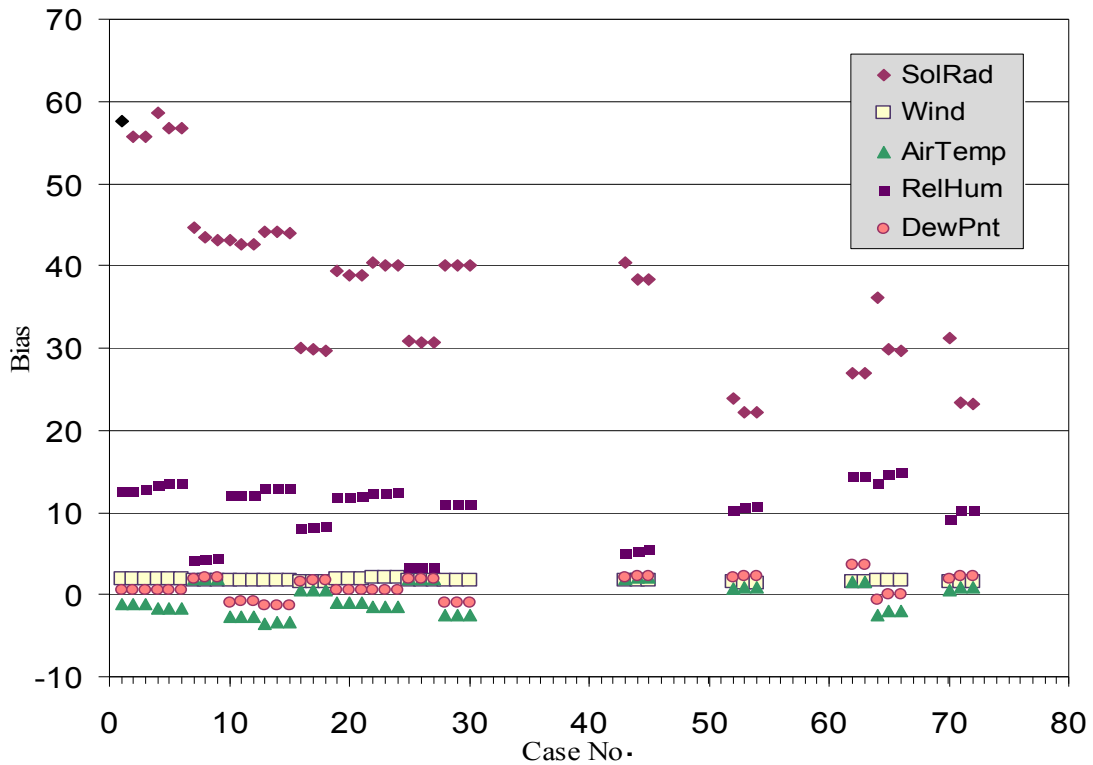


Figure 5: Plot of bias calculations for all cases analyzed for all variables

Table 4 shows a list of the cases that we identified as best and worst in simulating the various quantities accurately for the cases already examined in the study. Cases 65 and 66 show a remarkable potential in predicting everything except relative humidity and solar radiation. They give low correlation factors and high Rsme for these. They have a positive bias for all observed quantities except air temperature and dew point temperature. Surprisingly, case 64 which has all input variables the same except for the cumulus parameterization shows a different behavior. Obviously, these cases give the right values for the wrong reason. The number of snow layers in the Noah LSM is only one due to which the flux calculations are inaccurate and this shows up in the precipitation and relative humidity values. Also cases 65 and 66 show a correlation close to zero in total precipitation.

The in general bad correlation in precipitation could also be due to the method by which the terrain is modeled in WRF. Figure 6 shows the comparison between the actual terrain height and that assumed in the model at the 22 station locations. A maximum difference of 916 ft is found at Toklat and a minimum of 31 ft at Good pasture. When averaged over the 22 stations, this difference is 260ft.

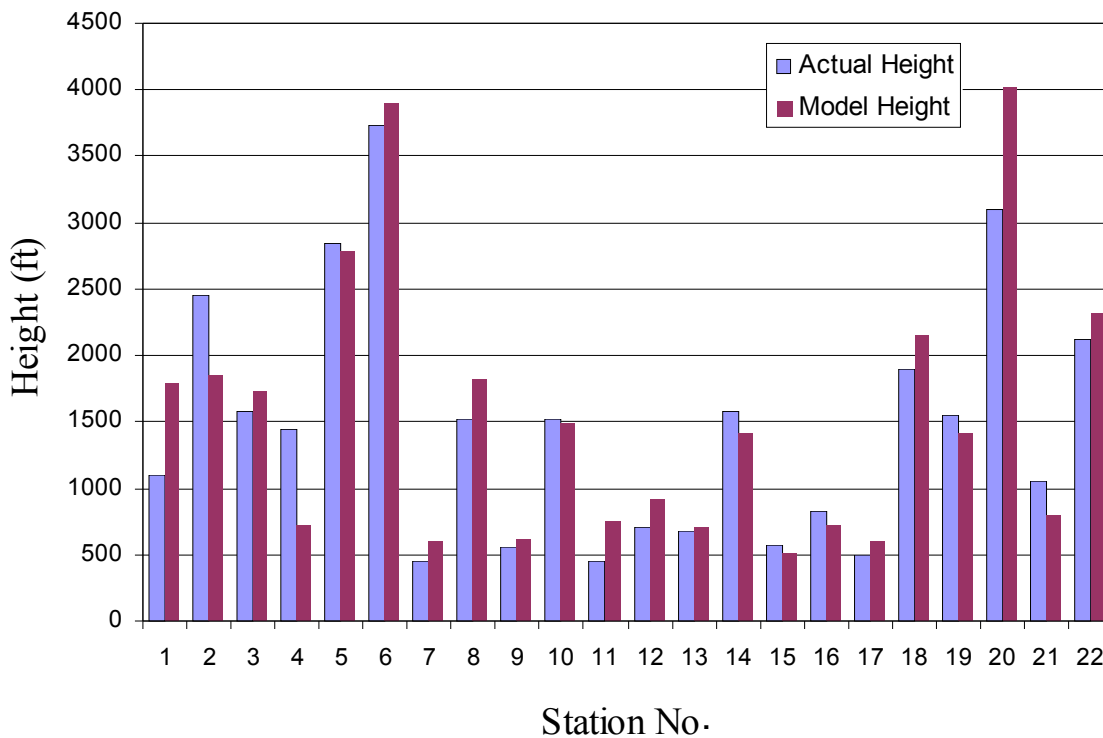


Figure 6: The terrain height used by the model compared with the actual height at each station.

Conclusion:

The preliminary results from the subset of simulations lead to the following conclusions: Based on the results shown in Figs. 4 and 5, along with results for the other variables and the average AWS statistics, we select the WRF configurations from cases 16, 17, 18 and 19, 20, 21 with the Ferrier microphysics, CAM scheme, Pleim-Xiu surface layer and boundary layer schemes and WSM 6-class graupel scheme microphysics, the unified Noah LSM respectively as the most suitable configuration for the case studied here. A forecaster has to use the output of several weather models to make a weather prediction as each model has its own strengths and weaknesses. It is possible that the best cases have not been simulated yet. Hence, the analysis will be more thorough and complete when all the 72 model configurations are compared and additional observational data are included in the evaluation. Furthermore, a detailed meteorological analysis is required why certain combination work better or worse. Here analysis of consistency in model physics has to be done by an experienced atmospheric scientist and modeler.

Scope for future:

The comparison can be made extensive by completing the simulations for the remaining cases of the seventy-two and maybe extended further to include other input options that haven't been varied so far. The simulation can be continued for another five days or another season to find the capability of WRF model to accurately predict weather over a longer period instead of just five. It would be interesting to see if the behavior of the various cases is any different if the correlation factor and Rsme are calculated for each individual station averaged over the entire 5 day period or averaged over a day. The results might be better if data from more weather stations in the domain are used for the comparison. Also, the stations where the actual terrain height and model height are very different can be omitted for the analysis to get a better view of the simulations.

Acknowledgment:

I am extremely thankful to Prof. Nicole Mölders who was my mentor for this project. I would like to thank Don Bahls, Alec Bennett, Jeremiah Dabney and the ARSC consult team for their support. I also appreciate the help, suggestions and encouragement rendered by S.E. Porter, M.E. Brown, D. PaiMazumder and my fellow interns. Last but not the least I would like to thank HPCMP and the JEOM Program office for giving me this wonderful opportunity to intern here and also ARSC for the computational resources.

References:

1. Brown, M.E., 2008. Impact of local external forcing of the 2006 Augustine Volcano eruption on regional weather conditions. MS Thesis, Dept. Atmos. Sci., University of Alaska Fairbanks, http://www.gi.alaska.edu/~molders/MEBrown_Thesis.pdf
2. Cheng, W.Y.Y., and W.J. Steenburgh, 2005: Evaluation of surface sensible weather forecasts by the WRF and the Eta models over the western United States. *Wea. Forecast.*, **20**, 812-821.
3. Collins, W.D. et al., 2004: Description of the NCAR Community Atmosphere Model (CAM 3.0), NCAR Technical Note, NCAR/TN-464+STR, 226
4. Davis, C., B. Brown, and R. Bullock, 2006: Object-based verification of precipitation forecasts. Part I: Methodology and application to mesoscale rain areas. *Mon. Wea. Rev.*, **134**, 1772-1784.
5. Done, J., C.A. Davis, and M. Weisman, 2004: The next generation of NWP: Explicit

- forecasts of convection using the weather research and forecasting (WRF) model. *Atmos. Sci. Lett.*, **5**, 110-117.
6. Dudhia, J., 1989: Numerical study of convection observed during the winter monsoon experiment using a mesoscale two-dimensional model. *J. Atmos. Sci.*, **46**, 3077-3107.
 7. Grell, G.A., S.E. Peckham, R. Schmitz, S.A. McKeen, G. Frost, W.C. Skamarock, and B. Eder, 2005: Fully coupled “online” chemistry within the WRF model. *Atmos. Environ.*, **39**, 6957-6975.
 8. Hines, K.M., D.H. Bromwich: Development and testing of polar weather research and forecasting (WRF) model. Part I: Greenland ice sheet meteorology, *Mon. Wea. Rev.*, **136**, 1971-1989
 9. Janjic, Z.I., 1994. The step-mountain eta coordinate model: further developments of the convection, viscous sublayer and turbulence closure schemes. *Mon. Wea. Rev.* **122**, 927-945.
 10. Janjic, Z.I., 1996. The surface layer in the NCEP Eta Model. Eleventh Conference on Numerical Weather Prediction, Norfolk, VA, 19-23 August 1996; Amer. Meteor. Soc., Boston, MA, 354-355.
 11. Janjic, Z.I., 2002. Nonsingular Implementation of the Mellor-Yamada Level 2.5 Scheme in the NCEP Meso model. NCEP Office Note No. 437, 61 pp.
 12. Kain, J.S., and Fritsch, J.M., 1990. A one-dimensional entraining/detraining plume model and its application in convective parameterization. *J. Atmos. Sci.*, **47**, 2784-2802.
 13. Kain, J.S., S.J. Weiss, J.J. Levit, M.E. Baldwin, and D.R. Brigh, 2006: Examination of convection-allowing configurations of the WRF model for the prediction of severe convective weather: The SPC/NSSL spring program 2004. *Wea. Forecast.*, **21**, 167-181.
 14. Knievel, J.C., D.A. Ahijevych, and K.W. Manning, 2004: Using temporal modes of rainfall to evaluate the performance of a numerical weather prediction model. *Mon. Wea. Rev.*, **132**, 2995-3009.
 15. Klemp, J.B., and W.C. Skamarock, 2004: Model numerics for convective-storm simulation. In: Fedorovich, E., R. Rotunno, and B. Stevens (Eds.), *Atmospheric turbulence and mesoscale meteorology*, Cambridge University Press, Cambridge, 117-137.
 16. Mölders, N., 2008. Suitability of the Weather Research and Forecasting (WRF) model to predict the June 2005 fire weather for Interior Alaska. *Wea. Forecast.* In press, pp. 21
 17. Morrison, H., Curry, J.A., Khvorostyanov, V.I., 2005. A new double-moment microphysics parameterization for application in cloud and climate models. Part I: Description. *J. Atmos. Sci.*, **62**, 1665-1677.

18. Noilhan, J., and Planton, S., 1989: A simple parameterization of land surface processes for meteorological models. *Mon. Wea. Rev.*, **117**, 536-549.
19. Otkin, J.A., T.J. Greenwald: Comparison of WRF model simulated and MODIS-derived cloud data, *Mon. Wea. Rev.*, **136**, 1957-1970.
20. Pleim, J.E., and Xiu, A., 2003. Development of a land surface model. Part II: Data assimilation. *J. Appl. Meteorol.*, **42**, 1811-1822.
21. Xiu, A., and Pleim, J.E., 2001. Development of a la